inhibitory neuron. About 2% of CA3 pyramidal cell targets are immunoreactive for parvalbumin. Thus, a pyramidal cell possessing 10–50 thousand boutons[18,29] may excite 200–1,000 parvalbumin-containing inhibitory cells. E.p.s.ps initiated by single pyramidal cells may cause inhibitory cell firing[9]. This excitatory drive presumably contributes to the high firing frequency of many hippocampal interneurons[11,14]. Thus the activation of a single CA3 pyramidal cell may, owing to high divergence in excitatory and inhibitory connections, disynaptically inhibit thousands of pyramidal cells in the CA3 and CA1 regions. This circuitry will operate in some, but not all, behavioural states to exert a strong, widespread inhibitory control of pyramidal cell firing[30]. □

Received 1 June; accepted 5 October 1993.

1. Heuser, J. E. & Reese, T. S. *Handbook of Physiology—The Nervous System* Vol. 1 (ed. Kandel, E. R.) 261–294 (Am. Phys. Soc., Bethesda, 1977).
2. Korn, H. & Faber, D. S. *Synaptic Function* (eds Edelman, G. M., Gall, W. E. & Cowan, W. M.) 57–108 (Wiley, New York, 1987).
3. Redman, S. *Physiol. Rev.* **70,** 165–198 (1990).
4. Stevens, C. F. *Neuron* **10,** 55–64 (1993).
5. Miles, R. & Wong, R. K. S. *J. Physiol.* **373,** 397–418 (1986).
6. Sayer, R. J., Redman, S. & Andersen, P. *J. Neurosci.* **9,** 840–850 (1989).
7. Malinow, R. *Science* **252,** 722–724 (1991).
8. Stern, P., Edwards, F. A. & Sakmann, B. *J. Physiol.* **449,** 247–278 (1992).
9. Miles, R. *J. Physiol.* **428,** 61–77 (1990).
10. Baimbridge, K. G., Miller, J. J. & Parkes, C. O. *Brain Res.* **239,** 519–525 (1982).
11. Kawaguchi, Y., Katsumaru, H., Kosaka, T., Heizmann, C. W. & Hama, K. *Brain Res.* **416,** 369–374 (1987).
12. Traub, R. D. & Miles, R. *Neuronal Networks of the Hippocampus* (Cambridge Univ. Press, UK, 1991).
13. Kosaka, T., Katsumaru, H., Hama, K., Wu, J. J. & Heizmann, C. W. *Brain Res.* **419,** 119–130 (1987).
14. Schwartzkroin, P. A. & Mathers, L. H. *Brain Res.* **157,** 1–10 (1978).
15. Hestrin, S. *Neuron* **9,** 991–999 (1993).
16. Bekkers, J. M., Richerson, G. B. & Stevens, C. F. *Proc. natn. Acad. Sci. U.S.A.* **87,** 5359–5362 (1990).
17. Tamamaki, N., Watanabe, K. & Nojyo, Y. *Brain Res.* **307,** 336–340 (1984).
18. Sik, A., Tamamaki, N. & Freund, T. F. *Eur. J. Neurosci.* (in the press).
19. Llinas, R., Bloedel, J. R. & Hillman, D. E. *J. Neurophysiol.* **32,** 847–870 (1969).
20. Somogyi, P., Kisvarday, Z. F., Martin, K. A. C. & Whitteridge, D. *Neuroscience* **10,** 261–294 (1983).
21. Freund, T. F., Martin, K. A. C., Somogyi, P. & Whitteridge, D. *J. comp. Neurol.* **242,** 275–291 (1985).
22. Busch, C. & Sakmann, B. *Cold Spring Harbor Symp.* **55,** 69–80 (1990).
23. Manabe, T., Renner, P. & Nicoll, R. A. *Nature* **355,** 50–55 (1992).
24. Raastad, M., Storm, J. F. & Andersen, P. *Eur. J. Neurosci.* **4,** 113–117 (1992).
25. Malgaroli, A. & Tsien, R. W. *Nature* **357,** 134–139 (1992).
26. McClelland, J. L. *et al. Parallel Distributed Processing* (MIT Press/Bradford Books, Massachusetts, 1986).
27. McNaughton, B. L. & Morris, N. G. *Trends Neurochem. Sci.* **10,** 408–415 (1987).
28. White, E. L. & Keller, A. *J. comp. Neurol.* **262,** 13–26 (1987).
29. Li, X. G., Somogyi, P., Ylinen, A. & Buzsáki, G. *J. comp. Neurol.* (in the press).
30. Buzsáki, G., Leung, L. W. S. & Vanderwolf, C. H. *Brain Res. Rev.* **6,** 139–171 (1983).

ACKNOWLEDGEMENTS. We thank G. Buzsáki for discussion and for comments on the manuscript, K. G. Baimbridge for antisera against parvalbumin, and E. Borók, I. Weisz, C. Pauletti and G. Terstyánszky for technical assistance. This work was supported by the Human Frontier Science Program Organization, the European Science Foundation, the Ministère de la Recherche et de la Technologie, the Hungarian Science Foundation, and OTKA Hungary.

Role of a metabotropic glutamate receptor in synaptic modulation in the accessory olfactory bulb

Yasunori Hayashi*†, Akiko Momiyama‡, Tomoyuki Takahashi‡§, Hitoshi Ohishi‖, Reiko Ogawa-Meguro‖, Ryuichi Shigemoto‖, Noboru Mizuno‖ & Shigetada Nakanishi*¶

* Institute for Immunology, † Department of Pharmacology, ‡ Department of Physiology, ‖ Department of Morphological Brain Science, Kyoto University Faculty of Medicine, Kyoto 606, Japan

VARIOUS functions of glutamate transmission are mediated by both ionotropic and metabotropic glutamate receptors[1]. The metabotropic glutamate receptors (mGluRs) consist of at least six different subtypes that are classified into three subgroups, mGluR1/mGluR5, mGluR2/mGluR3, and mGluR4/mGluR6 (refs 1–5), but their physiological roles are largely unknown. Here we report the identification of a very potent agonist for mGluR2/mGluR3, DCG-IV, and the specific localization of mGluR2 in granule cell dendrites that form dendrodendritic synapses with mitral cells in the accessory olfactory bulb. Using the DCG-IV agonist for mGluR2 in combination with slice patch-recording, we demonstrate that the granule cell mGluR2 presynaptically suppresses inhibitory GABA (γ-aminobutyrate) transmission to the mitral cell. Our results indicate that mGluR2 in granule cells plays an important role in the persistent excitation of olfactory sensory transmission in the accessory olfactory bulb by relieving mitral cells from the GABA inhibition.

Our previous study indicated that two extended L-isomers of 2-(carboxycyclopropyl)glycines (L-CCGs) are potent and selective agonists for the mGluR family[6]. An L-CCG derivative, (2S,1′R,2′R,3′R)-2-(2,3-dicarboxycyclopropyl)glycine (DCG-IV; Fig. 1) has recently been reported[7,8]. We determined agonist potencies of DCG-IV by examining its effects on the signal transduction of mGluR1, mGluR2, mGluR3 and mGluR4 expressed in Chinese hamster ovary (CHO) cells (Fig. 1). DCG-IV was a very potent agonist for both mGluR2 and mGluR3, with half-maximal effective concentrations (EC_{50}) of 3×10^{-7} M and 2×10^{-7} M, respectively. Remarkably, this compound had no obvious agonist activity for either mGluR1 or mGluR4. DCG-IV could bind to the NMDA (*N*-methyl-D-aspartate) receptor ($EC_{50}=3\times10^{-6}$ M) (Fig. 1) and induced an NMDA response ($EC_{50}\approx3\times10^{-5}$ M) in *Xenopus* oocytes expressing the cloned NMDA receptor (data not shown). Thus, the potency of DCG-IV for the NMDA receptors was at least one order of magnitude lower than that for the activation of mGluR2. DCG-IV had no antagonist activity on any mGluR subtypes, and did not interact with the α-amino-3-hydroxy-5-methyl-4-isoxazolepropionate-(AMPA)-kainate receptors. DCG-IV is thus a very useful agonist for mGluR2/mGluR3.

In situ hybridization analysis showed high expression of mGluR2 messenger RNA in limited regions of the rat brain[9] and particularly in granule cells of the accessory olfactory bulb (AOB) (Fig. 2*a*, *b*). We investigated the subcellular localization of mGluR2 in granule cells by using polyclonal antibody raised against the mGluR2 protein expressed in *Escherichia coli*. On western blot analysis, the mGluR2 antibody reacted with both mGluR2 and mGluR3 expressed individually in COS cells (Fig. 2*d*). This antibody gave rise to two bands representing mGluR2 and mGluR3 in membrane preparations from the cerebral cortex where mGluR3 mRNA is highly expressed[10]. In contrast, only the band corresponding to mGluR2 was observed in the AOB membrane preparation. mGluR3 mRNA is moderately expressed in mitral cells but not appreciably in granule cells of the AOB (ref. 10), indicating that the antibody crossreactivity with mGluR3 is weak. The mGluR2 antibody is thus useful for the subcellular localization of mGluR2 in granule cells.

In the AOB, mitral cells receive afferent inputs from the vomeronasal nerve and transmit excitatory outputs to various brain regions (Fig. 3*a*). Granule cells are inhibitory interneurons that form typical dendrodendritic synapses with mitral cells[11–13]. These synapses mediate reciprocal transmission in which the granule cell is excited by glutamate from the mitral cell and exerts an inhibition onto the mitral cell by GABA (refs 11–13).

§ Present address: Department of Neurophysiology, Institute for Brain Research, Faculty of Medicine, University of Tokyo, Tokyo 113, Japan.
¶ To whom correspondence should be addressed.

In electron microscopic analysis, the glutamatergic synapse can be seen as an asymmetric synapse where dense filamentous materials are located beneath the granule cell synaptic membrane and are confronted with spherical synaptic vesicles of the mitral cell[12,13]. The GABAergic synapse is seen as a symmetrical synapse where pleomorphic vesicles are localized under the membrane of the granule cell dendrite[12,13]. In immunoelectron microscopic analysis with the mGluR2 antibody, the localization of immunoreactivity of mGluR2 in granule cell dendrites was clearly seen (Fig. 2*c*). Furthermore, an immunopositive dendritic profile of a granule cell formed a synaptic contact with an immunonegative dendritic profile of a mitral cell (Fig. 2*c*).

On the basis of the above findings, we investigated the role of

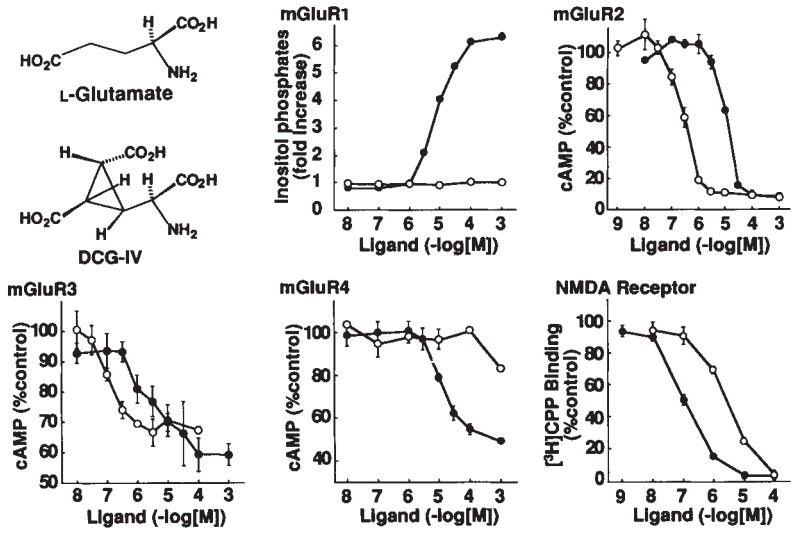

FIG. 1 Potencies and selectivity of DCG-IV for glutamate receptors. The total inositol phosphate formation was determined by incubating mGluR1-expressing CHO cells with test reagents for 20 min (ref. 6) and is expressed as multiples of inositol phosphate levels in agonist-untreated cells. Dose–response curves for inhibition of the forskolin-stimulated cAMP formation were determined by incubating mGluR2-, mGluR3- and mGluR4-expressing cells with test reagents in the presence of 10 μM forskolin for 10 min (ref. 6). cAMP levels in agonist-untreated cells are taken as 100%. Displacement curves of binding of [^{3}H]3-((±)-2-carboxypiperazin-4-yl)propyl-1-phosphate ([^{3}H]CPP, 10 nM) to the NMDA receptor were determined with crude synaptic membranes from adult rat forebrain in the absence (total binding) or presence (nonspecific binding) of 1 mM L-glutamate for 15 min on ice[17]. No appreciable binding of DCG-IV to the AMPA and kainate receptors were observed by similar displacement experiments using [^{3}H]AMPA (5 nM) and [^{3}H]kainate (2 nM), respectively[17]. ●, L-glutamate; ○, DCG-IV. Error bars are shown as the mean ± s.e.

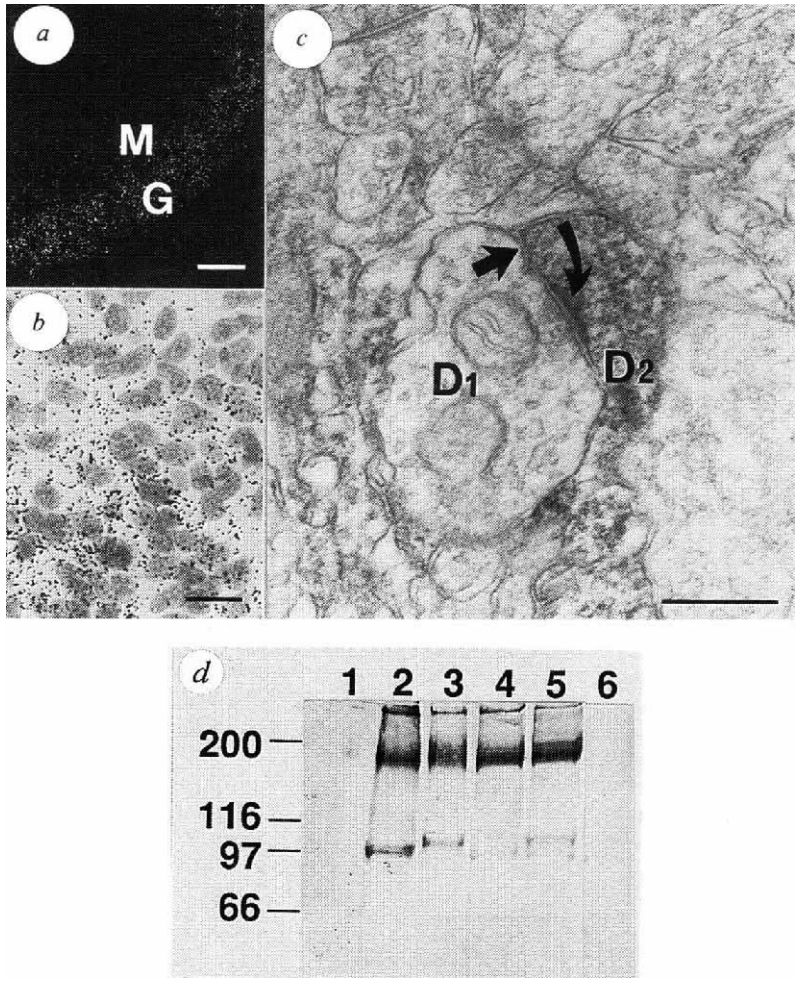

FIG. 2 Subcellular localization of mGluR2 in granule cells of the AOB. Dark- and bright-field photomicrographs of an emulsion-dipped section through the AOB of an 8-day-old rat are indicated in *a* and *b*, respectively. M, Mitral cell layer; G, granule cell layer. An electron micrograph (*c*) shows a dendrodendritic synapse between an immunonegative profile of a mitral cell dendrite (D_1) and an immunopositive profile of a granule cell dendrite (D_2) in the AOB of an adult rat. The D_2 is postsynaptic in an asymmetrical synapse (the curved arrow), and presynaptic in a symmetrical synapse (the straight arrow). Scale bars, 100 μm (*a*), 20 μm (*b*) and 0.5 μm (*c*). *d*, Immunoblot analysis of mGluR2 (~98K) and mGluR3 (~106K) was done with membrane fractions from the following sources: lane 1, non-transfected COS cells; lane 2, mGluR2-expressing COS cells; lane 3, mGluR3-expressing COS cells; lanes 4 and 6, AOB; and lane 5, cerebral cortex. In lane 6, the antibody was preabsorbed with a synthetic C-terminal peptide representing the antigen epitope of mGluR2. Positions of molecular mass (K) markers are indicated on the left.

METHODS. *In situ* hybridization was done using an *in vitro* synthesized, ^{35}S-labelled RNA probe corresponding to the 616-base-pair *Apa*I–*Sac*I fragment of the mGluR2 cDNA clone as described[2]. For the immunoelectron microscopic and immunoblot analyses, the construction, overexpression, purification and antibody production of the *trpE*-mGluR2 fusion protein were done as described[18]. The *trpE*-mGluR2 fusion protein containing a part of transmembrane segment VII and its following C-terminal portion of mGluR2 was made by inserting the 229-base-pair *Fok*I fragment of the mGluR2 cDNA into the *Eco*RI site of a pATH3 expression vector[18]. Immunoelectron microscopy of an AOB and immunoblot analysis of mGluR2 and mGluR3 were done using the affinity-purified antibody raised against mGluR2 according to the procedures described[18]. The higher-molecular-mass components probably represent polymeric aggregates of the receptor, because they were not observed with the preabsorbed antibody and were also stained inconsistently from experiment to experiment.

mGluR2 in synaptic transmission between the mitral cell and granule cell by examining the effect of DCG-IV on the GABA transmission to the mitral cell. Whole-cell recording was done from a mitral cell visually identified in thin slices at a holding potential of −70 mV (refs 14, 15) (Fig. 3*a*). The extracellular stimulation of a granule cell evoked an inward current (Fig. 3*b*). This response was blocked by the $GABA_A$-receptor antagonist bicuculline in a reversible manner (Fig. 3*b*). Also, when a mitral cell was electrically stimulated, a granule cell elicited excitatory postsynaptic currents that were sensitive to the AMPA/kainate receptor antagonist 6-cyano-7-nitroquinoxaline-2,3-dione (CNQX) (data not shown). We thus confirmed that the mitral

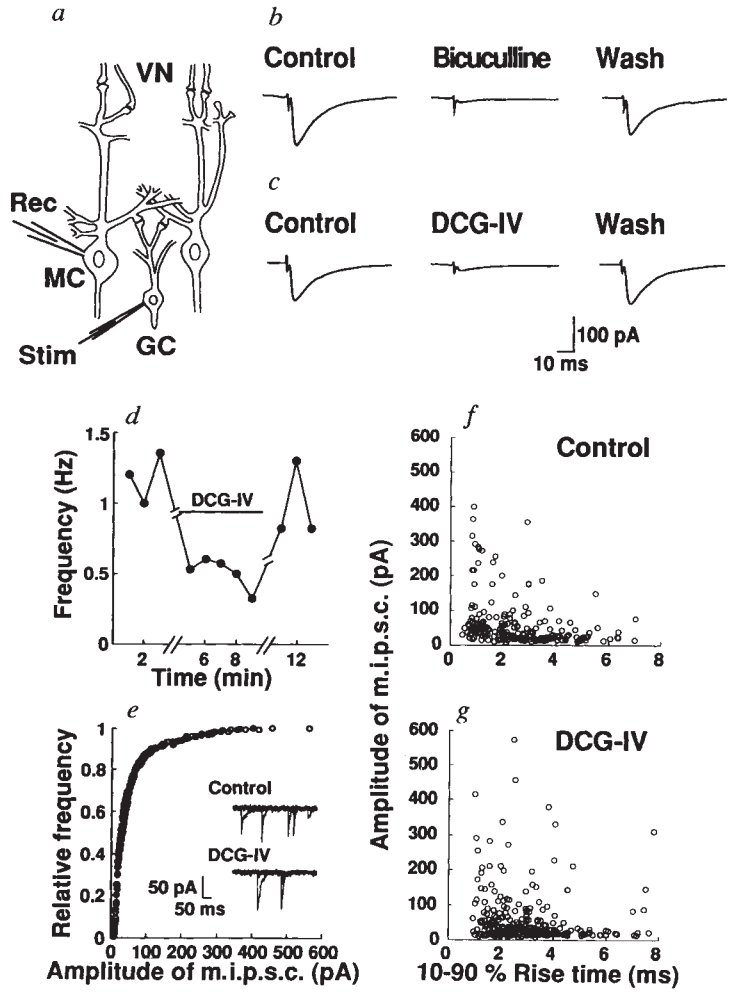

FIG. 3 Suppression of GABA-mediated i.p.s.cs by DCG-IV. As shown in *a*, whole-cell recording (Rec) of GABA-mediated i.p.s.cs was conducted by patch clamping of a cell body of a mitral cell (MC), and extracellular stimuli (Stim) were applied to a granule cell (GC) forming dendrodendritic synapses with the recorded mitral cell; VN, vomeronasal nerve. In *b* and *c*, current traces of GABA-mediated i.p.s.cs were recorded in the presence of 10 μM bicuculline and 3 μM DCG-IV, respectively. All traces are averaged records of 60 trials. Left traces, before drug application; middle traces, 90 s after drug application; right traces, after washing. The effect of DCG-IV on the frequency of m.i.p.s.cs is indicated in *d*. Each point represents the mean frequency of m.i.p.s.cs in a 1-min period. *e*, Cumulative probability distributions of amplitudes of spontaneous m.i.p.s.cs are plotted by recording mitral cells before (●; 219 events) and after application of 3 μM DCG-IV (○; 288 events), respectively. Miniature i.p.s.cs are shown in insets with 5 sweeps superimposed. There was no statistically significant difference in the two plots as assessed by the Kolmogorov–Smirnov test[19]. The rise time (10–90%)–amplitude relationships of m.i.p.s.cs before and after DCG-IV application are indicated in *f* and *g*, respectively. The mean rise times were 2.57 ms in the control and 2.93 ms in DCG-IV treatment.

METHODS. Coronal slices 130 μm-thick were prepared from 6–8-day-old rats using a tissue slicer in an oxygenated and chilled Krebs solution. Whole-cell recording from a mitral cell and stimulation of a granule cell were done by the slice patch-recording method[14,15]. The recording chamber was continuously perfused with a solution of the following compositions: 113 mM NaCl; 3 mM KCl; 1 mM NaH_2PO_4; 25 mM $NaHCO_3$; 11 mM glucose; 2 mM $CaCl_2$; 1 mM $MgCl_2$ (pH adjusted to 7.4 by bubbling with 95% O_2/5% CO_2); during recording, 0.5 μM strychnine and 10 μM CNQX were included in the perfusate[20]. The recording pipette contained a solution of the following compositions: 140 mM CsCl; 9 mM NaCl; 1 mM $MgCl_2$; 1 mM EGTA; 10 mM HEPES (pH adjusted to 7.3 with KOH). The pipette for stimulation was filled with 1 M NaCl and placed on a single granule cell. Miniature i.p.s.cs were recorded from mitral cells as described except that 0.3 μM tetrodotoxin was added to the perfusate.

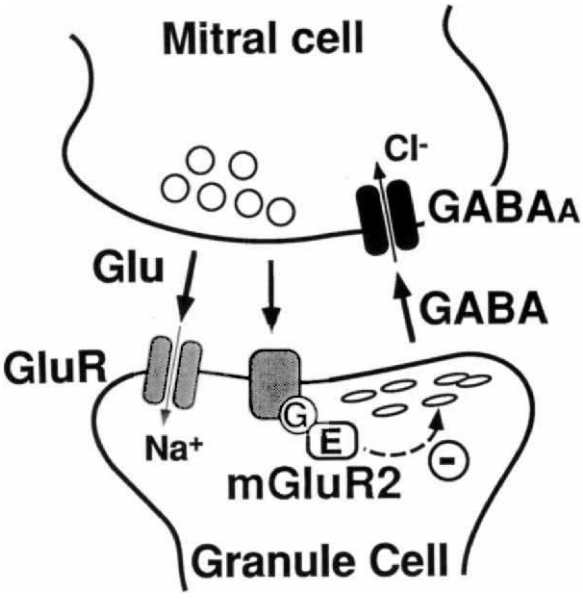

FIG. 4 A model of a modulatory role of mGluR2 in dendrodendritic synaptic transmission between a granule cell and a mitral cell. For detailed explanation, see text. The inhibition of GABA release is marked by a minus symbol but its mechanism remains unknown. GluR, ionotropic glutamate receptor; $GABA_A$, $GABA_A$ receptor; G, G protein; E, intracellular effector.

cells and the granule cells mediate reciprocal synaptic transmission. When DCG-IV was added to the perfusate, the amplitude of the GABA-mediated inhibitory postsynaptic current (i.p.s.c.) was markedly reduced (28.4 ± 15.3% of control levels; $n = 5$) in a reversible manner (Fig. 3*c*). At this drug concentration, no appreciable change was observed for the holding current. In this experiment, i.p.s.cs were measured in the perfusate containing 1 mM Mg^{2+} which blocks the NMDA receptors[16]. In addition, i.p.s.cs were inhibited to a similar extent (35.4 ± 26.3% of control levels; $n = 5$) in the presence of an NMDA receptor antagonist (50 μM D,L-2-amino-5-phosphonovalerate) (data not shown). Thus, the suppression of i.p.s.cs is not due to the action of DCG-IV on the NMDA receptors. We also confirmed that DCG-IV had no effect on mitral cell responses elicited by application of the $GABA_A$ receptor agonist muscimol (0.5 μM), and L-2-amino-4-phosphonobutyrate (50 μM), a potent mGluR4 subgroup agonist, had no effect on electrically evoked i.p.s.cs in mitral cells (data not shown). These results demonstrate that the activation of mGluR2 presynaptically suppresses a GABA inhibition on the mitral cell.

The presynaptic action of DCG-IV was further confirmed electrophysiologically by analysing spontaneous miniature i.p.s.cs (m.i.p.s.cs). DCG-IV suppressed the mean frequency of m.i.p.s.cs (62.7 ± 19.7% of control) without any change in either the cumulative probability of the amplitude distribution of m.i.p.s.cs or the rise time–amplitude relationship of m.i.p.s.cs before and after application of DCG-IV ($n = 3$) (Fig. 3*d–g*). In contrast, m.i.p.s.cs almost completely disappeared after application of bicuculline (data not shown). These results indicate that DCG-IV presynaptically reduces GABA release without changing postsynaptic responsiveness to GABA.

This study demonstrates that mGluR2 is present at the granule cell dendrites and presynaptically suppresses inhibitory GABA transmission to the mitral cell. Glutamate released from an excited mitral cell not only stimulates granule cells through the activation of the ionotropic glutamate receptor but also relieves the GABA-mediated inhibition onto the excited mitral cell through stimulation of mGluR2, as illustrated schematically in Fig. 4. The granule cell lacks an axon and forms divergent dendrodendritic synapses with a large number of surrounding mitral cells[11–13] (see also Fig. 3*a*). The excitation of mitral cells thus evokes lateral inhibition in the neighbouring mitral cells through trans-synaptically excited granule cells[11–13]. Under the mechanism revealed in this study, however, it can be postulated that the GABA inhibition is relieved in an excited mitral cell by the activation of mGluR2. Furthermore, this activation is thought to be confined to the synapses of the excited mitral cells and would thus maintain the lateral inhibition of unexcited neighbouring mitral cells. This mechanism would evidently enhance the signal-to-noise ratio between the excited mitral cells and their neighbouring mitral cells. The mGluR2-mediated modulation in the microcircuitry between the mitral cell and granule cell may be important in discrimination and resolution of the olfactory sensory transmission in the AOB. □

Received 29 June; accepted 6 October 1993.

1. Nakanishi, S. *Science* **258,** 597–603 (1992).
2. Masu, M., Tanabe, Y., Tsuchida, K., Shigemoto, R. & Nakanishi, S. *Nature* **349,** 760–765 (1991).
3. Houamed, K. M. *et al. Science* **252,** 1318–1321 (1991).
4. Tanabe, Y., Masu, M., Ishii, T., Shigemoto, R. & Nakanishi, S. *Neuron* **8,** 169–179 (1992).
5. Abe, T. *et al. J. biol. Chem.* **267,** 13361–13368 (1992).
6. Hayashi, Y. *et al. Br. J. Phamac.* **107,** 539–543 (1992).
7. Ohfune, Y., Shimamoto, K., Ishida, M. & Shinozaki, H. *Bioorg. med. Chem. Lett.* **3,** 15–18 (1993).
8. Ishida, M., Saitoh, T., Shimamoto, K., Ohfune, Y. & Shinozaki, H. *Br. J. Pharmac.* **109,** 1169–1177 (1993).
9. Ohishi, H., Shigemoto, R., Nakanishi, S. & Mizuno, N. *Neuroscience* **53,** 1009–1018 (1993).
10. Ohishi, H., Shigemoto, R., Nakanishi, S. & Mizuno, N. *J. comp. Neurol.* **335,** 252–266 (1993).
11. Rall, W. & Shepherd, G. M. *J. Neurophysiol.* **31,** 884–915 (1968).
12. Mori, K. *Prog. Neurobiol.* **29,** 275–320 (1987).
13. Shepherd, G. M. *Sci. Am.* **238,** 92–103 (1978).
14. Edwards, F. A., Konnerth, A., Sakmann, B. & Takahashi, T. *Pflügers Arch.* **414,** 600–612 (1989).
15. Takahashi, T. *J. Physiol., Lond.* **450,** 593–611 (1992).
16. Moriyoshi, K. *et al. Nature* **354,** 31–37 (1991).
17. Kawai, M., Horikawa, Y., Ishihara, T., Shimamoto, K. & Ohfune, Y. *Eur. J. Pharmac.* **211,** 195–202 (1992)
18. Shigemoto, R. *et al. Neurosci. Lett.* **153,** 157–160 (1993).
19. Van der Kloot, W. *Prog. Neurobiol.* **36,** 93–130 (1991).
20. Ito, S. & Cherubini, E. *J. Physiol., Lond.* **440,** 67–83 (1991).

ACKNOWLEDGEMENTS. We thank Y. Ohfune and K. Shimamoto for DCG-IV, M. Kuno for advice and A. Uesugi for photographic assistance. Partly supported by research grants from the Ministry of Education, Science and Culture of Japan, the Ministry of Health and Welfare of Japan and the Senri Life Science Foundation.

A *Drosophila* homologue of human Sp1 is a head-specific segmentation gene

Ernst A. Wimmer*†, Herbert Jäckle†, Christine Pfeifle*‡ & Stephen M. Cohen*‡

* Howard Hughes Medical Institute, Department of Cell Biology, Baylor College of Medicine, Houston, Texas 77030, USA
† Abteilung Molekulare Entwicklungsbiologie, Max-Planck-Institut für biophysikalische Chemie, Postfach 2841, D-37018 Göttingen, Germany

SEGMENTATION in *Drosophila* is based on a cascade of hierarchical gene interactions initiated by maternally deposited morphogens that define the spatially restricted domains of gap gene expression at blastoderm (reviewed in ref. 1). Although segmentation of the embryonic head is morphologically obscured, the repeated patterns of expression of the segment polarity genes reflect the formation of seven head segments[2,3]; two of these depend on the segmentation and homeotic genes used in the trunk, whereas the others form as a result of the activity of the head-specific genes *orthodenticle* (*otd*), *empty spiracles* (*ems*) and *buttonhead* (*btd*). The genes *ems* and *otd* encode homeodomain proteins, suggesting that they may function as transcription factors[4–6]. They are expressed in overlapping stripes in the early embryonic head of *Drosophila*, and their vertebrate homologues, *otx* and *emx*, are expressed in overlapping domains in the anterior central nervous system of the mouse embryo[7,8]. We show here that *btd* is expressed in a stripe covering the head anlagen of the segments affected in *btd* lack-of-function mutants and that *btd* encodes a zinc-finger-type transcription factor with sequence and functional similarity to the prototype mammalian transcription factor Sp1 (ref. 9). When expressed in the spatial pattern of *btd*, a transgene providing Sp1 activity can support development of the mandibular segment in the head of *btd* mutant embryos. A ubiquitous transcription factor from humans can therefore replace an essential component of the genetic circuitry required to specify the development of a particular head segment in the fly.

Positional cloning of the *btd* locus was initiated using a yeast artificial chromosome (YAC) clone[10] (Fig. 1). The identification of the *btd* gene is based on a 10.5-kilobase (kb) transgene which can rescue the *btd* mutant phenotype, and on DNA sequences

‡ Present address: European Molecular Biology Laboratory, Postfach 102209, D-69012 Heidelberg, Germany